Amine-Borane Dehydropolymerization using Rh-based Pre-Catalysts: Resting State, Chain-Control and Efficient Polymer Synthesis.

David E. Ryan,[a,b] Kori A. Andrea,[c] James J. Race,[a,b] Timothy M. Boyd,[a,b] Guy C. Lloyd–Jones[d] and Andrew S. Weller*[a]

[a] Department of Chemistry, University of York, Heslington, York, YO10 5DD (UK)

[b] Department of Chemistry, Chemical Research Laboratories, University of Oxford, Oxford, OX1 3TA (UK)

[c] Department of Chemistry, Memorial University of Newfoundland, St. John's, Newfoundland, A1B 3X7 (Canada)

[d] School of Chemistry, University of Edinburgh, Edinburgh, EH9 3FJ (UK)

Keywords: Dehydropolymerization, Rhodium, Phosphine, Mechanism, Amine-borane

A detailed study of $H_3B \cdot NMeH_2$ dehydropolymerization using the cationic pre-catalyst [Rh(DPEphos)($H_2BNMe_3(CH_2)_2^tBu$)][BAr$^F_4$], identifies the resting state as dimeric [Rh(DPEphos)H_2]$_2$ and boronium [$H_2B(NMeH_2)_2$]$^+$ as the chain-control agent. [Rh(DPEphos)H_2]$_2$ can be generated in situ from Rh(DPEphos)(benzyl), and catalyzes polyaminoborane formation (H_2BNMeH)$_n$ [M_n = 15000 g mol^{-1}]. Closely-related Rh(Xantphos)(benzyl) operates at 0.1 mol%, to give higher molecular weight polymer [M_n = 85000 g mol^{-1}] on gram scale with low residual [Rh], 81 ppm. This insight offers a mechanistic template for dehydropolymerization.

The catalyzed dehydropolymerization of amine-boranes, archetypically $H_3B \cdot NMeH_2$, is an atom-efficient methodology for the synthesis of polyaminoboranes (H_2BNRH)$_n$ (Scheme 1A), forming H_2 as the only by-product.[1-4] This new class of main-group polymer[5] is based upon BN main-chain units, and is isosteric with technologically-mature polyolefins. These main-chain B–N units suggest, in addition to unexplored material and chemical properties, potential applications as piezoelectric materials,[6,7] or as precursors to boron-based ceramics and *h*-BN.[1,8,9]

Scheme 1. (A) Amine–Borane Dehydropolymerization, (B) Exemplar Pre-Catalyst Systems.

(A) Amine-borane dehydropolymerization
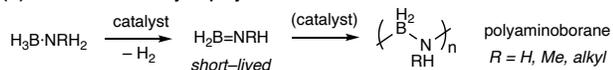
(B) Exemplar pre-catalysts
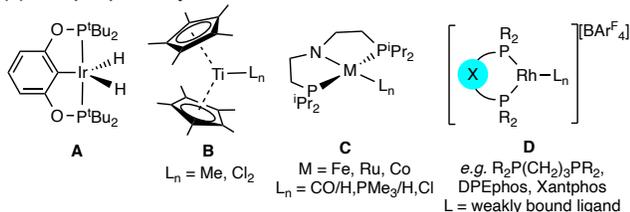
The currently accepted overarching mechanism for polymer formation from amine-borane involves initial dehydrogenation to form a transient[10] aminoborane ($H_2B=NRH$), that then undergoes end-chain nucleophilic B–N bond formation, initiated by the catalyst.[3,11-16] While non-catalytic routes have been reported,[10,17] in terms of overall efficiency, scalability, substrate scope, and control of the polymer characteristics, catalytic routes offer the broadest opportunity for the tailored synthesis of polyaminoboranes.

A wide range of pre-catalyst systems have been described for amine-borane dehydropolymerization (Scheme 1B). After the original report of high[3] molecular weight polymer formed using Ir(POCOP)H_2 **A** [POCOP = κ^3-1,3-($^tBu_2PO$)$_2C_6H_3$],[1,11] systems based on group-4 metallocenes **B**,[18,19] cooperative ligands **C**,[14,16,20,21] and cationic [RhL$_2$]$^+$ pre-catalysts (L$_2$ = e.g., Ph$_2$P(CH$_2$)$_3$PPh$_2$, DPEphos, Xantphos) **D**,[22-24] have been described. For the Rh-based catalysts we have reported speciation, kinetics and degree of polymerization studies. These are broadly generalized by: an induction period, a non-living chain-growth propagation, an inverse relationship between catalyst loading and degree of polymerization, and H_2 acting as a chain controlling agent to reduce polymer chain length,[15,22-24] Scheme 2.

Scheme 2: Exemplar Complex 1 and Prior Observations.

General Observations
Chain–growth mechansim
Induction period
H_2 lowers M_n
Increasing [cat] lowers M_n

Added NMeH$_2$
Removes induction period
Increases M_n
[cat]$^{0.5}$
$\delta(^{31}P)$ = 41 during catalysis

This work
Kinetic, speciation and synthesis studies

Leads to

Active catalyst, chain–control agents, targeted synthesis of new catalysts, control of dehydropolymerization
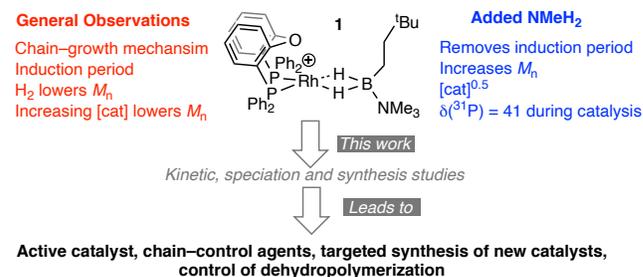
We have also reported on the key role of NMeH$_2$, formed by B–N bond cleavage in $H_3B \cdot NMeH_2$.[21,25] Exemplified using the [Rh(DPEphos)($H_2BNMe_3CH_2CH_2^tBu$)][BAr$^F_4$] pre-catalyst,[23]

1 [Ar^F = 3,5-(CF$_3$)$_2$C$_6$H$_3$], the amine NMeH$_2$ removes the induction period, increases the degree of polymerization, and simplifies the kinetics, allowing a half order dependency on [Rh]$_{TOTAL}$ to be determined. However, the structure of the active catalyst is undetermined, with insight limited to the detection of a single species at δ(^{31}P) 41.3 [J(RhP) = 150 Hz]. Also lacking is a robust explanation for the relationship between [Rh]$_{TOTAL}$, and H$_2$, on the degree of polymerization.

Despite these advances, the precise details of initiation, propagation and termination remain to be determined for these diverse catalyst systems,[3] while identification of resting states is rare[14,16] and challenging.[18] Herein we report on an investigation of the [Rh(DPEphos)]$^+$ pre-catalyst system, **1**, in which a study of the kinetics, speciation and synthesis has allowed identification of the active catalyst, as well as allowing for the polymer-growth/termination processes to be interrogated. These insights are then harnessed in the design of a new, efficient, Rh-based catalyst that produces polyaminoborane on scale. A simple protocol is also described to significantly reduce the levels of residual catalyst in the isolated polymer.

We have previously reported that when **1** is employed as pre-catalyst, the monocationic hydrido-aminoborane dimer [Rh$_2$(DPEphos)$_2$(μ-H)(μ-H$_2$B=NHMe)][BAr$^F_4$] **2** is formed during the early stages of reaction.[23] We propose this arises via an amine-promoted B–H hydride transfer[26] in a precursor cationic σ-amine borane complex [Rh(DPEphos)(H$_3$B·NMeH$_2$)][BAr$^F_4$], **E**,[27] to generate a neutral hydride of empirical formula Rh(DPEphos)H (Scheme 3). Similar hydride species are formed in [Rh(PONOP)(H$_3$B·NMe$_2$H)]$^+$ [25] and [Rh(^{i}Pr$_2$P(CH$_2$)$_3$P^{i}Pr$_2$)-(H$_3$B·NH$_3$)]$^+$ [28] systems, alongside H$_2$B=NMe$_2$/[NMe$_2$H$_2$]$^+$ or boronium [H$_2$B(NH$_3$)$_2$]$^+$ respectively. Based on these observations, a simple kinetics model was constructed for the induction process, involving generation of **2** by rapid trapping of Rh(DPEphos)H with unreacted **E**, followed by a slow, amine-dependent, fragmentation to form the active catalyst. This telescopes the elementary steps of the induction process,[29] allows H$_2$ evolution to be used as proxy for transient H$_2$B=NMeH, and successfully reproduces the temporal concentration profiles,[23] as a function of [Rh]$_{TOTAL}$ (0.2 and 0.4 mol%), or when NMeH$_2$ is added; Scheme 3. A VTNA analysis[30,31] supports the observation of an empirical fractional order in pre-catalyst: [Rh]$_{TOTAL}^{0.5}$.

Scheme 3. Model and Fitted data.[23] [BAr$^F_4$]$^-$, DPEphos Not Shown. [H$_3$B·NMeH$_2$] = 0.223 M (1,2–F$_2$C$_6$H$_4$).
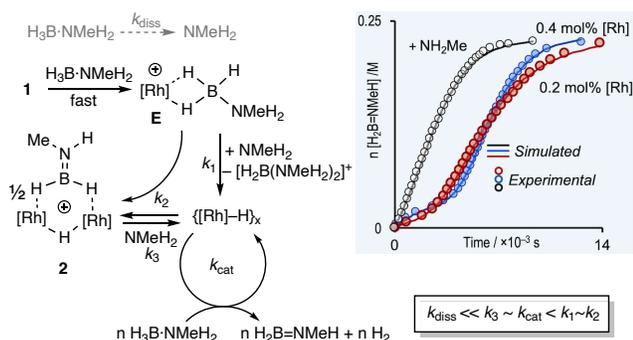
With an effective model for the induction process determined, we then focussed on identification of the catalyst

resting state. Based on our model, and the work of Fryzuk[32,33] and Tilley,[34] the neutral hydride bridged dimer [Rh(DPEphos)H$_2$]$_2$, **3**, was synthesized in situ, by addition of either H$_2$ or H$_3$B·NMeH$_2$ to the new benzyl complex Rh(κ^2–P,P–DPEphos)(η^3-H$_2$CPh) **4**, Scheme 4. Toluene is formed in all cases. The 298K ^{31}P{^{1}H} NMR data for **3** match that observed during catalysis, i.e. δ 41.3 [J(RhP) = 150 Hz, d^8–THF]. The hydride ligands in **3** are fluxional at 298 K, presenting a very broad signal at δ –8.1. Cooling to 253 K reveals three environments at δ –6.9 (2H), –9.9 (1H) and –17.5 (1H). This pattern is similar to those reported for Rh$_2$L$_4$H$_4$ [L = P(O^{i}Pr)$_3$, ½ ^{i}Pr$_2$P(CH$_2$)$_3$P^{i}Pr$_2$],[32,35] and is indicative of three bridging hydrides and one terminal hydride. The ^{31}P{^{1}H} NMR spectrum of **3** at 253 K was poorly resolved, showing multiple, mutually-coupled, signals.

Scheme 4. Synthesis and Reactivity of Complex 3. [BAr$^F_4$]$^-$ Not Shown.
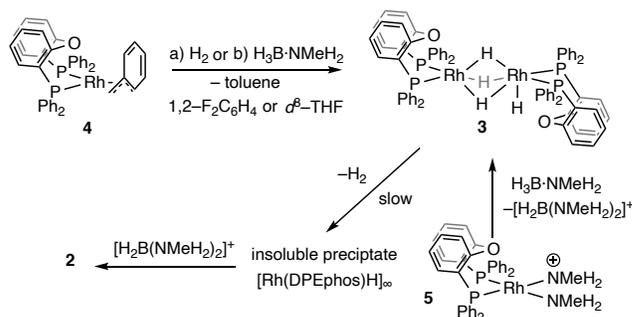
Addition of excess H$_3$B·NMeH$_2$ to the amine complex [Rh(DPEphos)(NMeH$_2$)$_2$][BAr$^F_4$], **5**,[23] also generates **3**, together with boronium [H$_2$B(NMeH$_2$)$_2$]$^+$ [δ(^{11}B) –7.8]. Solutions of complex **3** in 1,2–F$_2$C$_6$H$_4$, or in THF, irreversibly lose H$_2$ on degassing, to form an insoluble yellow/brown powder, analyzing as [Rh(DPEphos)H]$_\infty$, likely to be a coordination polymer with Rh–H–Rh linkages. While the Rh-polymer does not dissolve on addition of H$_2$, the soluble complex **2** is regenerated when [H$_2$B(NMeH$_2$)(OEt$_2$)][BAr$^F_4$] is added.[10] Thus, when using a cationic pre-catalyst (i.e. **1** or **5**), persistent NMeH$_2$ will favor soluble neutral hydride via equilibration with complex **2** (k_3, Scheme 3). When using neutral pre-catalyst **4**, a high initial concentration of amine-borane, e.g. [H$_3$B·NMeH$_2$]$_0$ = 0.446 M in THF, inhibits the formation of a precipitate. Presumably, the amine-borane intercepts Rh(DPEphos)H before it oligomerizes. Thus, dimeric, neutral, hydride **3** is observed as the common resting state, irrespective of the pre-catalyst, or solvent. The half order dependence in [Rh]$_{TOTAL}$ points to a rapid endergonic equilibrium between dimer and monomer, prior to the turn-over limiting step. This has been noted in other Rh$_2$H$_x$ systems,[32,36,37] and the data are thus consistent with the resting state being dimeric **3**. An important difference between neutral versus cationic pre-catalysts, is that the latter generate a boronium co-product, which has important implications for the dehydropolymerization, as discussed next.

Neutral pre-catalyst **4** was deployed in the dehydropolymerization of H$_3$B·NMeH$_2$ at a variety of catalyst loadings, Table 1. Using 1,2–F$_2$C$_6$H$_4$ as the solvent, kinetics measurements were hampered by formation of the insoluble precipitate. In THF, eudiometric measurements on H$_2$ production were less reliable due to solvent volatility. Nevertheless,

Table 1 GPC Characterization Data[a]

Entry	Cat.	[Rh]$_{TOTAL}$ (mol%)	M_n [M_p] (g mol^{-1})[b]	Đ	[boronium] (mol%)
1	**4**	0.25	15000	2.5	0
2	**4**	0.5	15000	2.5	0
3	**4**	1	15000 [35000]	2.4	0
4	**4**[c]	0.5	17000	2.3	0
5	**4**[c]	1	17000	2.4	0
6	**4**	1	[25000]	n/a	0.25
7	**4**	1	[21000]	n/a	0.5
8	**4**	1	[<19000][d]	n/a	1
9	**6**	1	88000	1.5	0
10	**6**	1	21000	1.5	1
11	**6**[c,e]	0.1	85000	1.5	0
13	**7**	1	98000	1.6	0

[a] 298 K, 1,2–F$_2$C$_6$H$_4$, 0.223 M H$_3$B·NMeH$_2$, isobaric conditions under flow of Ar, end point determined by ^{11}B NMR spectroscopy. [b] Relative to polystyrene standards; triple column; RI detection; THF with 0.1 w/w % [NBu$_4$]Br; 35 °C; [sample] = 2 mg cm^{-3}. [c] THF solvent. [d] M_p of the polymer distribution obscured by [BAr$^F_4$]$^-$ signal. [e] 5 M, 1.1 g scale.

polymerization goes to completion in both solvents, selectively forming [H$_2$BNMeH]$_n$, Figure 1A.[38] A plot of conversion versus M_n (Figure 1B, relative to polystyrene standards)[3,11,16] is characteristic of a non-living chain-growth polymerization: at low conversions the polymer is formed with high M_n and H$_3$B·NMeH$_2$ dominates. Variations in catalyst loading did not affect the degree of polymerization of the resulting polyaminoborane, in either 1,2–F$_2$C$_6$H$_4$ (Figure 1C, M_n = 15000 g mol^{-1}) or THF solutions (M_n = 17000 g mol^{-1}), under 'open conditions' with a slow Ar-flow. This is different to cationic pre-catalysts, such as **1**, where M_n scales inversely with [Rh]$_{TOTAL}$: e.g. 6400 (1 mol%), 34900 g mol^{-1} (0.2 mol%).[23] However, 'closed conditions' that allow for build–up of H$_2$ result in very low molecular weight oligomers being formed (1 mol % **4**, less than 1000 gmol^{-1} by GPC, ^{11}B NMR spectroscopy[31]). The cationic pre-catalyst **1** behaves analogously.[22]

The neutral and cationic pre-catalyst systems differ by the presence of a boronium co-product with the latter, the relative concentration of which will scale with [Rh]$_{TOTAL}$.[39] Given the underlying insensitivity to the degree of polymerization to [Rh]$_{TOTAL}$ when using neutral **4**, we thus considered whether with cationic pre-catalysts boronium [H$_2$B(NMeH$_2$)$_2$][BAr$^F_4$] can act as a chain-control agent to modify M_n. To test this, [H$_2$B(NMeH$_2$)$_2$][BAr$^F_4$] was doped (0.25 to 1 mol%) into 1 mol% **4** / H$_3$B·NMeH$_2$, to selectively form polyaminoborane (^{11}B NMR). Although GPC analysis of the resulting polymer using refractive index detection is affected by the co-eluting [BAr$^F_4$]$^-$ masking the lower molecular weight region (Figure 1D),[15] there is a qualitative trend of decreasing M_p with increasing [H$_2$B(NMeH$_2$)$_2$][BAr$^F_4$], Table 1. This outcome is consistent with boronium acting as a chain-control agent. Chain Length Distribution (ln–CLD) analysis of high molecular weight fractions in GPC has been
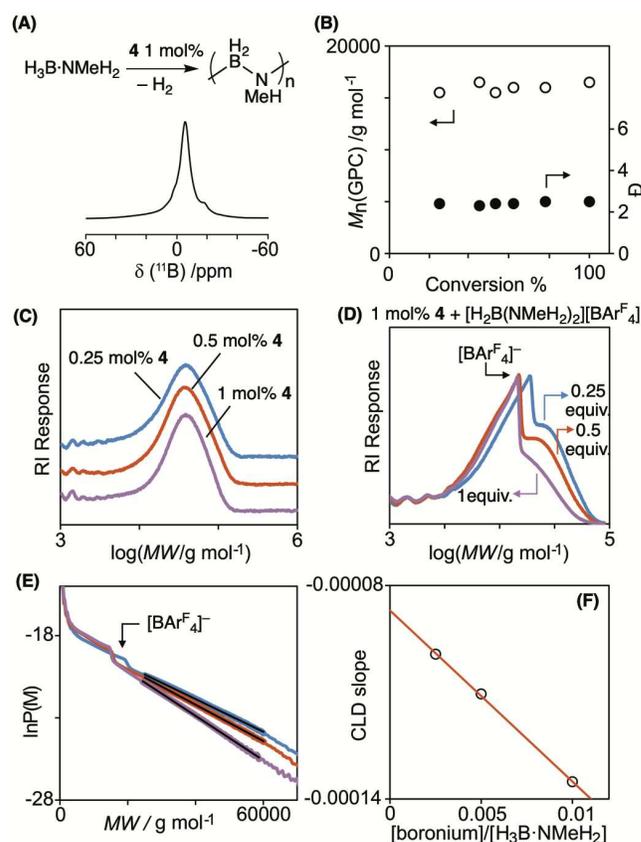

Figure 1. Polyaminoborane data obtained using catalyst 4 (Ar flow, 1,2–F$_2$C$_6$H$_4$, H$_3$B·NMeH$_2$ = 0.223 M) (A) ^{11}B NMR spectrum of polymer; (B) M_n versus conversion; (C) GPC data for 1.0, 0.5 and 0.25 mol% catalyst loadings; (D) GPC data for 1.0 mol% 4 with [H$_2$B(NMeH$_2$)$_2$][BAr$^F_4$] doping. (E) ln–CLD plot of high M_w fraction (D). (F) Mayo analysis.

shown to be useful where there is overlap between distributions of polymer and transfer agents, such as that noted here, allowing for chain control processes to be probed.[40] A Mayo-type plot of [boronium]/[H$_3$B·NMeH$_2$] versus the ln–CLD slope indicates an inversely linear relationship (Figure 1E and F), further supporting the conclusion that the boronium functions as a rapid chain control agent in the dehydropolymerization.

Collectively, the analysis above facilitates the construction of a mechanistic landscape for dehydropolymerization, Scheme 5, that is consistent not only with the results herein, but also with our previous observations on cationic Rh-based systems.[15,22,23,28,41] Thus, dehydrogenation of amine-borane to give the reactive monomer, H$_2$B=NMeH, occurs at a neutral [Rh–H] species, in an H$_2$-mediated equilibrium with dimer **3**. Dehydrogenation to form H$_2$B=NMeH, via BH/NH activation (Scheme 5A) could be facilitated by a hemilabile DPEphos ligand (e.g. κ^2 and κ^3 coordination[42]) as previously suggested.[43] Initiated by a formal hydride-transfer from the rhodium hydride,[44] that is now playing a dual role in both dehydrogenation and initiation,[11,14] H$_2$B=NMeH then undergoes rapid head-to-tail end-chain nucleophilic B–N bond formation, as proposed previously (Scheme 5B).[12,13,15,16] Chain-control by protonation of the terminal nucleophilic amine of the polymeryl group by boronium returns a cationic pre-catalyst, aminoborane and NMeH$_2$, that

3

Scheme 5. Proposed (A) Catalyst Evolution/Dehydrogenation, (B) Propagation, (C) Chain–Control Events.

Figure 2. (A) New pre-catalysts, (B) Representative reaction, (C) Isolated polymer and (D) GPC trace [cat. = 5, 0.1 mol%].
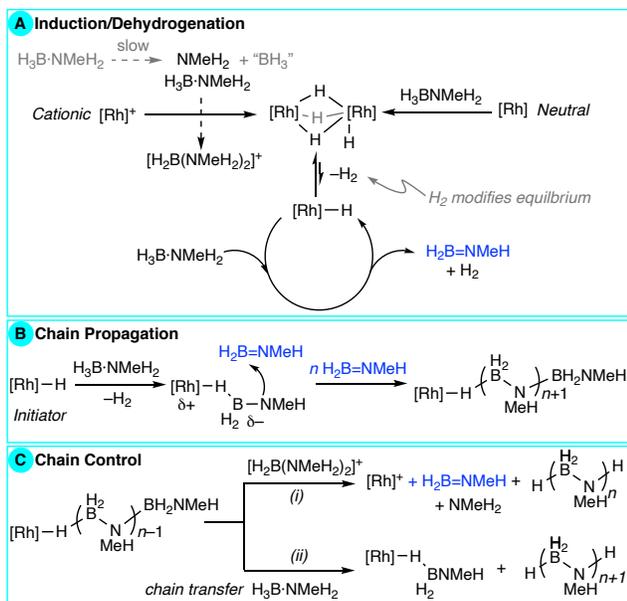
are rapidly recycled (Scheme 5C).[25] A related intramolecular proton transfer has been proposed by Paul and co-workers for Ir(POCOP)H$_2$ systems.[13] We speculate that, in the absence of boronium, chain transfer to pre-monomer H$_3$B·NMeH$_2$ controls chain-length, Scheme 5C. Whatever the precise mechanism for these chain-control processes, they result in relatively narrow dispersities of the final isolated polymer, as a result of the constant degrees of polymerization during the entire reaction (Figure 1B).[45] H$_2$ loss from **3**, and related systems,[32,35] occurs readily on degassing. The position of the initial monomer/dimer equilibrium is thus expected to be sensitive to [H$_2$], impacting on the rate of dehydrogenation as well initiator concentration. This, we suggest, is the origin of the low degrees of polymerization observed under 'closed conditions'. In support of this, for a system where hydride-bridged dimer formation is disfavoured due to sterics, e.g. Rh(Xantphos-^{i}Pr)H, H$_2$ does not act to modify the degree of polymerization.[15] The precise gearing of all of these interconnected relationships is therefore pre-catalyst, co-product (e.g. boronium) and solvent specific.

The use of new pre-catalysts based upon neutral **4** demonstrates wider applicability, and also signal the opportunity for the exploitation of structure/activity relationships (Figure 2, Table 1). For example, the Xantphos benzyl complex, **6**, is an effective pre-catalyst for dehydropolymerization (1 mol%, 88000 g mol^{-1}, Đ 1.6), and the degree of polymerization can be controlled by [H$_2$B(NMeH$_2$)$_2$][BArF$_4$], e.g. 1 mol% M_n = 21000 g mol^{-1}. Complex **6** can be used at low loadings and high [H$_3$B·NMeH$_2$] (0.1 mol%, 5 M in THF, using commercially sourced amine-borane), to produce high[3] molecular weight polyaminoborane on gram scale (85000 g mol^{-1}, 1.1 g). Use of activated charcoal in the polymer work-up reduces the [Rh]-content from 195 ppm (no workup) to 81 ppm. This is considerably lower than reported for other Rh and Co dehydropolymerization systems.[15,21,46] The simple benzyl-dppp-catalyst **7** also promotes formation of high molecular weight polyaminoborane (98000 g mol^{-1}).
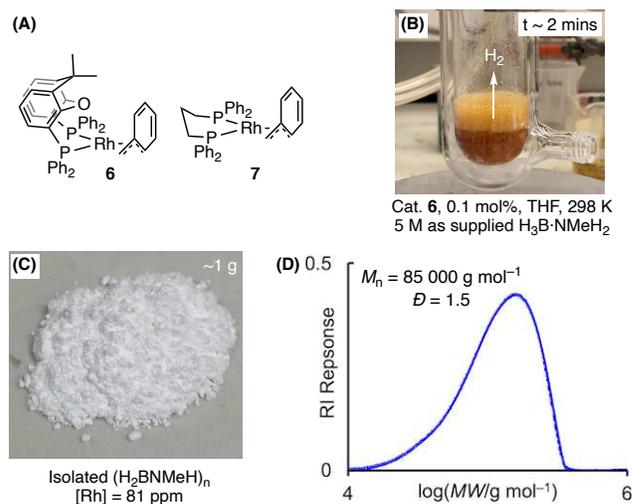
In summary, the identification of the catalyst resting state, the events that lead to its formation, and thus the role that co-products such as boronium and H$_2$ likely play in chain-control, have provided important insights into the complex and nuanced set of interconnected processes that are required for selective amine-borane dehydropolymerization using Rh(bisphosphine)-based catalysts. While the detailed elucidation of the elementary steps awaits further study, Scheme 5 provides a testable framework for the analysis and design of catalyst systems for controlled amine-borane dehydropolymerization.

ASSOCIATED CONTENT

Supporting Information

Full experimental, structural, kinetics data and details of the simulated model. The Supporting Information is available free of charge on the ACS Publications website.

AUTHOR INFORMATION

Corresponding Author

* andrew.weller@york.ac.uk

Author Contributions

The manuscript was written through contributions of all authors

REFERENCES

(1) Staubitz, A.; Presa Soto, A.; Manners, I. Iridium-Catalyzed Dehydrocoupling of Primary Amine–Borane Adducts: A Route to High Molecular Weight Polyaminoboranes, Boron–Nitrogen Analogues of Polyolefins. *Angew. Chem. Int. Ed.* **2008**, *47*, 6212-6215.

(2) Leitao, E. M.; Jurca, T.; Manners, I. Catalysis in service of main group chemistry offers a versatile approach to p-block molecules and materials. *Nature Chem.* **2013**, *5*, 817-829.

(3) Colebatch, A. L.; Weller, A. S. Amine–Borane Dehydropolymerization: Challenges and Opportunities. *Chem. Eur. J.* **2019**, *25*, 1379-1390.

(4) Han, D.; Anke, F.; Trose, M.; Beweries, T. Recent advances in transition metal catalysed dehydropolymerisation of amine boranes and phosphine boranes. *Coord. Chem. Rev.* **2019**, *380*, 260-286.

(5) Vidal, F.; Jäkle, F. Functional Polymeric Materials Based on Main-Group Elements. *Angew. Chem. Int. Ed.* **2019**, *58*, 5846-5870.

(6) Nakhmanson, S. M.; Nardelli, M. B.; Bernholc, J. Ab Initio Studies of Polarization and Piezoelectricity in Vinylidene Fluoride and BN-Based Polymers. *Phys. Rev. Lett.* **2004**, *92*, 115504.

(7) Zhang, Y.; Hopkins, M. A.; Liptrot, D. J.; Khanbareh, H.; Groen, P.; Zhou, X.; Zhang, D.; Bao, Y.; Zhou, K.; Bowen, C. R.; Carbery, D. R. Harnessing Plasticity in an Amine-Borane as a Piezoelectric and Pyroelectric Flexible Film. *Angew. Chem. Int. Ed.* **2020**, *59*, 7808-7812.

(8) Du, V. A.; Jurca, T.; Whittell, G. R.; Manners, I. Aluminum borate nanowires from the pyrolysis of polyaminoborane precursors. *Dalton Trans.* **2016**, *45*, 1055-1062.

(9) Wang, X.; Hooper, T. N.; Kumar, A.; Priest, I. K.; Sheng, Y.; Samuels, T. O. M.; Wang, S.; Robertson, A. W.; Pacios, M.; Bhaskaran, H.; Weller, A. S.; Warner, J. H. Oligomeric aminoborane precursors for the chemical vapour deposition growth of few-layer hexagonal boron nitride. *CrystEngComm* **2017**, *19*, 285-294.

(10) Metters, O. J.; Chapman, A. M.; Robertson, A. P. M.; Woodall, C. H.; Gates, P. J.; Wass, D. F.; Manners, I. Generation of aminoborane monomers RR'N–BH$_2$ from amine–boronium cations [RR'NH–BH$_2$L]$^+$: metal catalyst-free formation of polyaminoboranes at ambient temperature. *Chem. Commun.* **2014**, *50*, 12146-12149.

(11) Staubitz, A.; Sloan, M. E.; Robertson, A. P. M.; Friedrich, A.; Schneider, S.; Gates, P. J.; Schmedt auf der Günne, J.; Manners, I. Catalytic Dehydrocoupling/Dehydrogenation of N-Methylamine-Borane and Ammonia-Borane: Synthesis and Characterization of High Molecular Weight Polyaminoboranes. *J. Am. Chem. Soc.* **2010**, *132*, 13332-13345.

(12) Baker, R. T.; Gordon, J. C.; Hamilton, C. W.; Henson, N. J.; Lin, P.-H.; Maguire, S.; Murugesu, M.; Scott, B. L.; Smythe, N. C. Iron Complex-Catalyzed Ammonia–Borane Dehydrogenation. A Potential Route toward B–N-Containing Polymer Motifs Using Earth-Abundant Metal Catalysts. *J. Am. Chem. Soc.* **2012**, *134*, 5598-5609.

(13) Bhunya, S.; Malakar, T.; Paul, A. Unfolding the crucial role of a nucleophile in Ziegler–Natta type Ir catalyzed polyaminoborane formation. *Chem. Commun.* **2014**, *50*, 5919-5922.

(14) Glüer, A.; Förster, M.; Celinski, V. R.; Schmedt auf der Günne, J.; Holthausen, M. C.; Schneider, S. Highly Active Iron Catalyst for Ammonia Borane Dehydrocoupling at Room Temperature. *ACS Catal.* **2015**, *5*, 7214-7217.

(15) Adams, G. M.; Colebatch, A. L.; Skornia, J. T.; McKay, A. I.; Johnson, H. C.; Lloyd–Jones, G. C.; Macgregor, S. A.; Beattie, N. A.; Weller, A. S. Dehydropolymerization of H$_3$B·NMeH$_2$ To Form Polyaminoboranes Using [Rh(Xantphos-alkyl)] Catalysts. *J. Am. Chem. Soc.* **2018**, *140*, 1481-1495.

(16) Anke, F.; Boye, S.; Spannenberg, A.; Lederer, A.; Heller, D.; Beweries, T. Dehydropolymerisation of methylamine borane and an N-substituted primary amine borane using a PNP Fe catalyst. *Chem. Eur. J.* **2020**, *10.1002/chem.202000809*.

(17) De Albuquerque Pinheiro, C. A.; Roiland, C.; Jehan, P.; Alcaraz, G. Solventless and Metal-Free Synthesis of High-Molecular-Mass Polyaminoboranes from Diisopropylaminoborane and Primary Amines. *Angew. Chem. Int. Ed.* **2018**, *57*, 1519-1522.

(18) LaPierre, E. A.; Patrick, B. O.; Manners, I. Trivalent Titanocene Alkyls and Hydrides as Well-Defined, Highly Active, and Broad Scope Precatalysts for Dehydropolymerization of Amine-Boranes. *J. Am. Chem. Soc.* **2019**, *141*, 20009-20015.

(19) Jurca, T.; Dellermann, T.; Stubbs, N. E.; Resendiz-Lara, D. A.; Whittell, G. R.; Manners, I. Step-growth titanium-catalysed dehydropolymerisation of amine–boranes. *Chem. Sci.* **2018**, *9*, 3360-3366.

(20) Knitsch, R.; Han, D.; Anke, F.; Ibing, L.; Jiao, H.; Hansen, M. R.; Beweries, T. Fe(II) Hydride Complexes for the Homogeneous Dehydrocoupling of Hydrazine Borane: Catalytic Mechanism via DFT Calculations and Detailed Spectroscopic Characterization. *Organometallics* **2019**, *38*, 2714-2723.

(21) Boyd, T. M.; Andrea, K. A.; Baston, K.; Johnson, A.; Ryan, D. E.; Weller, A. S. A simple cobalt-based catalyst system for the controlled dehydropolymerisation of H$_3$B·NMeH$_2$ on the gram-scale. *Chem. Commun.* **2020**, *56*, 482-485.

(22) Johnson, H. C.; Leitao, E. M.; Whittell, G. R.; Manners, I.; Lloyd-Jones, G. C.; Weller, A. S. Mechanistic Studies of the Dehydrocoupling and Dehydropolymerization of Amine–Boranes Using a [Rh(Xantphos)]$^+$ Catalyst. *J. Am. Chem. Soc.* **2014**, *136*, 9078-9093.

(23) Adams, G. M.; Ryan, D. E.; Beattie, N. A.; McKay, A. I.; Lloyd-Jones, G. C.; Weller, A. S. Dehydropolymerization of H$_3$B·NMeH$_2$ Using a [Rh(DPEphos)]$^+$ Catalyst: The Promoting Effect of NMeH$_2$. *ACS Catal.* **2019**, *9*, 3657-3666.

(24) Colebatch, A. L.; Hawkey Gilder, B. W.; Whittell, G. R.; Oldroyd, N. L.; Manners, I.; Weller, A. S. A General, Rhodium-Catalyzed, Synthesis of Deuterated Boranes and N-Methyl Polyaminoboranes. *Chem. Eur. J.* **2018**, *24*, 5450-5455.

(25) Spearing-Ewyn, E. A. K.; Beattie, N. A.; Colebatch, A. L.; Martinez-Martinez, A. J.; Docker, A.; Boyd, T. M.; Baillie, G.; Reed, R.; Macgregor, S. A.; Weller, A. S. The role of neutral Rh(PONOP)H, free NMe$_2$H, boronium and ammonium salts in the dehydrocoupling of dimethylamine-borane using the cationic pincer [Rh(PONOP)(η^2-H$_2$)]$^+$ catalyst. *Dalton Trans.* **2019**, *48*, 14724-14736.

(26) Roselló-Merino, M.; López-Serrano, J.; Conejero, S. Dehydrocoupling Reactions of Dimethylamine-Borane by Pt(II) Complexes: A New Mechanism Involving Deprotonation of Boronium Cations. *J. Am. Chem. Soc.* **2013**, *135*, 10910-10913.

(27) See Supporting Materials for model complex for **E** : [Rh(κ^2-P,P-DPEphos)(η^{2}η^2-H$_3$B·NMe$_3$)][BAr$^F_4$].

(28) Kumar, A.; Beattie, N. A.; Pike, S. D.; Macgregor, S. A.; Weller, A. S. The Simplest Amino-borane H$_2$B=NH$_2$ Trapped on a Rhodium Dimer: Pre-Catalysts for Amine–Borane Dehydropolymerization. *Angew. Chem. Int. Ed.* **2016**, *55*, 6651-6656.

(29) These will be defined and discussed in a future contribution.

(30) Nielsen, C. D. T.; Burés, J. Visual kinetic analysis. *Chem. Sci.* **2019**, *10*, 348-353.

(31) See Supporting Materials

(32) Fryzuk, M. D.; Piers, W. E.; Einstein, F. W. B.; Jones, T. Coordinatively unsaturated binuclear clusters of rhodium. The reactivity of [{Pr$^i_2$P(CH$_2$)$_n$PPr$^i_2$}Rh]$_2$(μ-H)$_2$ (n = 2, 3, and 4) with dihydrogen, and their use in the catalytic hydrogenation of olefins. *Can. J. Chem.* **1989**, *67*, 883-896.

(33) Fryzuk, M. D.; H.McConville, D.; Rettig, S. J. Synthesis, structure and hydrogenation of η^3-benzyl diphosphine complexes of rhodium and iridium. *J. Organomet. Chem.* **1993**, *445*, 245-256.

(34) Han, L.-B.; Tilley, T. D. Selective Homo- and Heterodehydrocouplings of Phosphines Catalyzed by Rhodium Phosphido Complexes. *J. Am. Chem. Soc.* **2006**, *128*, 13698-13699.

(35) Sivak, A. J.; Muetterties, E. L. Metal clusters. 21. Synthesis of rhodium phosphite clusters. *J. Am. Chem. Soc.* **1979**, *101*, 4878-4887.

(36) Kumar, A.; Ishibashi, J. S. A.; Hooper, T. N.; Mikulas, T. C.; Dixon, D. A.; Liu, S.-Y.; Weller, A. S. The Synthesis, Characterization and Dehydrogenation of Sigma-Complexes of BN-Cyclohexanes. *Chem. Eur. J.* **2016**, *22*, 310-322.

(37) Brown, J. M.; Lloyd-Jones, G. C. Vinylborane Formation in Rhodium-Catalyzed Hydroboration of Vinylarenes. Mechanism versus Borane Structure and Relationship to Silation. *J. Am. Chem. Soc.* **1994**, *116*, 866-878.

(38) Monitoring by NMR spectroscopy (1 mol%, THF, closed system) shows no induction period.

(39) Some neutral pre-catalyst systems may also produce co-products that scale with [cat], such as boronium or ammonium, through amine-promoted M–Cl for M–H metathesis. See ref 21.

(40) Moad, G.; Moad, C. L. Use of Chain Length Distributions in Determining Chain Transfer Constants and Termination Mechanisms. *Macromol.* **1996**, *29*, 7727-7733.

(41) Dallanegra, R.; Robertson, A. P. M.; Chaplin, A. B.; Manners, I.; Weller, A. S. *Chem. Commun.* **2011**, *47*, 3763.

(42) Adams, G. M.; Weller, A. S. POP-type ligands: Variable coordination and hemilabile behaviour. *Coord. Chem. Rev.* **2018**, *355*, 150-172.

(43) Esteruelas, M. A.; Nolis, P.; Oliván, M.; Oñate, E.; Vallribera, A.; Vélez, A. Ammonia Borane Dehydrogenation Promoted by a Pincer-Square-Planar Rhodium(I) Monohydride: A Stepwise Hydrogen Transfer from the Substrate to the Catalyst. *Inorg. Chem.* **2016**, *55*, 7176-7181.

(44) Addy, D. A.; Bates, J. I.; Kelly, M. J.; Riddlestone, I. M.; Aldridge, S. Aminoborane σ Complexes: Significance of Hydride Co-ligands in Dynamic Processes and Dehydrogenative Borylene Formation. *Organometallics* **2013**, *32*, 1583-1586.

(45) Chain-capping events have been discussed in phosphine-borane dehydropolymerization. Oldroyd, N.L.; Chitnis, S. S.; Annibake, V. T.; Arz, M. I.; Sparkes, H. A.; Manners, I. Metal-free dehydropolymerisation of phosphine-boranes using cyclic (alkyl)(amino)carbenes as hydrogen acceptors *Nature Commun.* **2019**, *10*, 1370

(46) Turner, J. R.; Resendiz-Lara, D. A.; Jurca, T.; Schäfer, A.; Vance, J. R.; Beckett, L.; Whittell, G. R.; Musgrave, R. A.; Sparkes, H. A.; Manners, I. Synthesis, Characterization, and Properties of Poly(aryl)phosphinoboranes Formed via Iron-Catalyzed Dehydropolymerization. *Macromol. Chem. Phys* **2017**, *218*, 1700120.

ToC